Improving light trapping and conversion efficiency of amorphous silicon solar cell by modified and randomly distributed ZnO nanorods*

Jia Zhi-Nan(贾志楠)[a)b)], Zhang Xiao-Dan(张晓丹)[a)†], Liu Yang(刘 阳)[a)], Wang Yan-Feng(王延峰)[a)], Fan Jun(樊 君)[a)c)], Liu Cai-Chi(刘彩池)[b)], and Zhao Ying(赵 颖)[a)]

[a)] *Institute of Photo-Electronics Thin Film Devices and Technology of Nankai University, Key Laboratory of Photo-Electronics Thin Film Devices and Technology of Tianjin, Tianjin* 300071, *China*

[b)] *School of Materials Science and Engineering, Hebei University of Technology, Tianjin* 300130, *China*

[c)] *School of Information and Engineering, Hebei University of Technology, Tianjin* 300130, *China*

(Received 14 July 2013; revised manuscript received 9 October 2013; published online 20 February 2014)

Three-dimensional (3D) nanostructures in thin film solar cells have attracted significant attention due to their applications in enhancing light trapping. Enhanced light trapping can result in more effective absorption in solar cells, thus leading to higher short-circuit current density and conversion efficiency. We develop randomly distributed and modified ZnO nanorods, which are designed and fabricated by the following processes: the deposition of a ZnO seed layer on substrate with sputtering, the wet chemical etching of the seed layer to form isolated islands for nanorod growth, the chemical bath deposition of the ZnO nanorods, and the sputtering deposition of a thin Al-doped ZnO (ZnO:Al) layer to improve the ZnO/Si interface. Solar cells employing the modified ZnO nanorod substrate show a considerable increase in solar energy conversion efficiency.

Keywords: random ZnO nanorod, light trapping Al-doped ZnO, solar cells

PACS: 61.46.Km, 78.35.+c, 77.55.hf, 88.40.H– **DOI:** 10.1088/1674-1056/23/4/046106

1. Introduction

Thin film solar cells with a three-dimensional (3D) nanostructure have a potential advantage in improving light trapping and promoting charge separation,[1–3] which are both primary routes to the enhancement of solar cell efficiency. Among the manufacturing processes of solar cells with a 3D nanostructure, the fabrication of nano-textured substrates plays a key role. There have been several studies demonstrating that highly ordered nanoscale textures can dramatically increase the performance of light absorption in thin-film solar cells.[4,5] However, in order to fabricate such highly ordered nanostructures, various kinds of nano-scale masks, such as silica nanospheres,[4] Sn nanospheres,[5] polystyrene nanospheres,[6,7] and anodic alumina oxide,[8] must be used.

Recently, Battaglia *et al.*[9] showed that thin film solar cells deposited on randomly and periodically distributed nano-structured substrates exhibit almost the same performance in both theory and experiment. This research suggests that we can fabricate a substrate with a random 3D structure, which may lead to better light trapping in thin film solar cells than in the cells on planar substrates, but does not need the introduction of any highly ordered masks. Furthermore, Lin *et al.*[10] have also reported that the randomly nano-structured solar cells show good performance because of improved light coupling.

In various nanostructures, ZnO nanorods have attracted considerable attention because they have a strong chemical self-assemble ability[11] and are easy to grow using many methods, including catalyst-initiated epitaxy,[12] thermal chemical vapor deposition,[13,14] electro-deposition,[15] and solution chemistry methods.[16–19] The thin film solar cells have also been deposited on ZnO nanostructure arrays.[20,21] Among these growth methods, the solution chemistry method has the following advantages: 1) both the equipment and the reagent are cost effective; 2) the operation process is relatively easy and convenient; and, 3) a large size substrate can be obtained in production. However, in traditional wet chemical solution methods that are used to grow ZnO nanorods, the nanorods are usually too closely packed, so it is difficult to obtain high quality silicon thin film solar cells with 3D structures. In this study, we grow ZnO nanorods that are randomly distributed in different intervals between nanorods. The key innovation is to etch the sputtered ZnO layer to form isolated islands, which will be the seeds to grow ZnO nanorods. In the process, we fabricated ZnO nanorods without using any mask, and the space between nanorods can be changed by changing

*Project supported by the National Basic Research Program of China (Grant Nos. 2011CBA00706 and 2011CBA00707), the High-Technology Research and Development Program of China (Grant No. 2013AA050302), the Science and Technology Support Program of Tianjin City, China (Grant No. 12ZCZDGX03600), the Major Science and Technology Support Project of Tianjin City, China (Grant No. 11TXSYGX22100), and the Specialized Research Fund for the Ph. D. Program of Higher Education, China (Grant No. 20120031110039).

†Corresponding author. E-mail: xdzhang@nankai.edu.cn

© 2014 Chinese Physical Society and IOP Publishing Ltd

the etching time. In order to improve the interface, a sputtered ZnO:Al (AZO) layer is made to cover the surface of the ZnO nanorods, which will be referred to as modified ZnO nanorods below. We make the hydrogenated amorphous silicon (a-Si:H) solar cells on the modified ZnO nanorod coated glass substrates. For comparison, the solar cells are also made of regular ZnO nanorod coated glass substrates and planar ZnO coated glass substrates. The solar cells on the modified ZnO nanorod coated glass substrates show an obvious improvement in the light trapping and energy conversion efficiency.

2. Experimental details

First, we cleaned the glass substrates thoroughly using a sequence of acetone, isopropanol, ethanol, and DI water. Second, we deposited a $\sim$ 200-nm thick seed layer on the substrate using a direct current (DC) magnetron sputtering of an Al doped (0.5 wt%) ZnO ceramic target. Third, we chemically etched the substrates by immersing them in a 1-M NaOH solution at room temperature for different times. Fourth, we synthesized ZnO nanorods by floating the substrate on the nutrient solution surface, which was composed of a 15-mM solution with a 1:1 ratio zinc nitrate hexahydrate ($Zn(NO_3)_2.6H_2O$) and hexamethylenetramine ($(CH_2)_6N_4$) at 90 °C for 40 min. The specimens were mounted upside-down on beakers (200 mL) to prevent any precipitates that formed in the nutrient solution from falling onto the substrates, which would inhibit the growth of the nanorods.[16] The samples were then rinsed with DI water and ethanol, alternately, several times to remove any residual organics, and then dried by nitrogen gas. Finally, we sputtered a 180-nm thick AZO layer on the top of each ZnO nanorod to improve the interface between the ZnO and a-Si:H layers.

After the substrates were fabricated, we deposited a-Si:H solar cells in a multi-chamber system with plasma-enhanced chemical vapor deposition. The depositions of the p, i, and n layers were made consecutively on the substrates to form p–i–n structured solar cells, where p, i, n represent the p-type, intrinsic, and n-type semiconductors, respectively. The i layer was prepared using SiH_4 and H_2. $B(CH_3)_3$ and PH_3 were used for p-type and n-type doping, respectively. Evaporated Al dots were used to form the back contact and define the area of the cells. The active area of the cell was 0.253 cm^2. The whole fabrication process of the 3D solar cells is schematically demonstrated in Fig. 1.

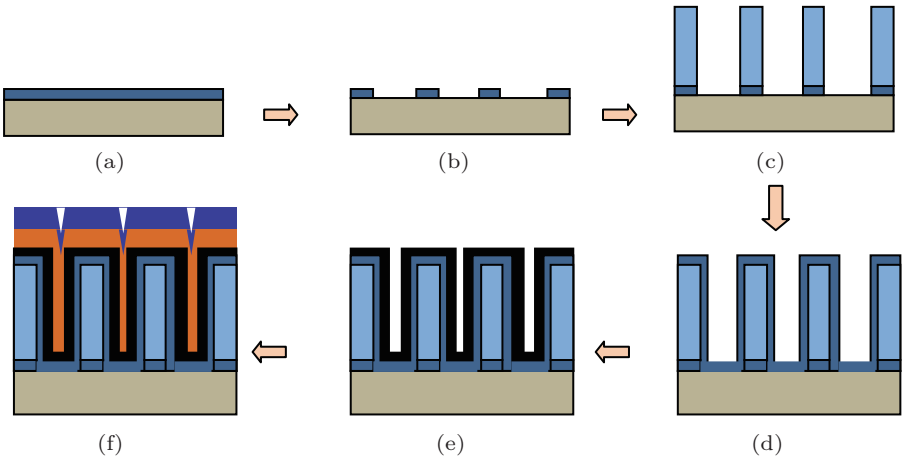


Fig. 1. (color online) Schematic diagrams of the 3D solar cells fabrication process: (a) sputtering ZnO:Al seed layer on ITO glass; (b) etching the seed layer by NaOH solution; (c) growing ZnO nanorod arrays by wet chemical method; (d) sputtering ZnO:Al thin film on the surfaces of ZnO nanorods; (e) PECVD- deposited a-Si:H p–i–n stack layers; (f) LPCVD-deposited and heat-evaporated 90-nm ZnO:B and 500-nm Al sequentially.

The open circuit voltage (V_{oc}) and fill factor (FF) of the solar cells were calculated from the current versus voltage (J–V) characteristic curve measured in the standard test condition of 25 °C, global air mass 1.5 (AM1.5G) spectra, and 100 mW/cm^2 of light intensity. External quantum efficiency (EQE) spectra were measured under zero electrical bias. The short circuit current density (J_{sc}) was calculated by convolution integral of the EQE and the photon flux of the AM1.5G spectrum. A field emission scanning electron microscope (SEM) was used to investigate the morphologies of the samples. The surface morphologies and roughness sizes of the films were also characterized by atomic force microscopy (AFM, NanoNavi-SPA400). Optical reflectance and transmittance measurements were carried out using a photo spectrometer equipped with an integrating sphere on a larger area sample of 15 mm^2 to improve the signal-to-noise ratio.

3. Results and discussion

In the case of using a wet chemical method, ZnO nanorods are often prepared through two steps. First, a ZnO

seed layer template is usually made using a physical vapor deposition, such as sputtering. Second, ZnO nanorods are grown on the seed layer using a chemical method. The seed layer has been found to strongly affect the geometries and orientations of the nanorods grown on the top of the seed layer.[22] The seed layer is able to reduce the energy of nucleation, and thus the nanorods only grow in the areas with the seed layer. Considering the significant effect that the seed layer exerts on the growth of the ZnO nanorods, we deposited an AZO seed layer using a sputtering method and adjusted the spacing between the ZnO nanorods by wet-etching the seed layer for different times. An AZO seed layer of about 200-nm was deposited on an ITO coated glass substrate. Then, we immersed the sample into a 1-M NaOH solution at room temperature for different times. Figures 2(a1)–2(a3) show the surface morphologies of seed layers after 5 min, 10 min, and 15 min of etching, respectively. The areas of the seed layer coverage became smaller as etching time increased. We grew ZnO nanorods on the seed layers with different etching times. Figures 2(b1)–2(b3) show the effects of seed layer size on the distribution of nanorods. The longer the etching time, the larger the spacing between the nanorods was. This proves that the spacing between the ZnO nanorods can be adjusted by etching the seed layer for different times. Compared with the mask-using method, this method is easy to operate and inexpensive. We sputtered a layer of AZO thin film as a covering layer on the surface of the ZnO nanorods. Figures 2(c1)–2(c3) show that the morphologies of the substrates are changed from nanorods with sharp edges and corners, to nanocones (modified nanorods) after the AZO coating.

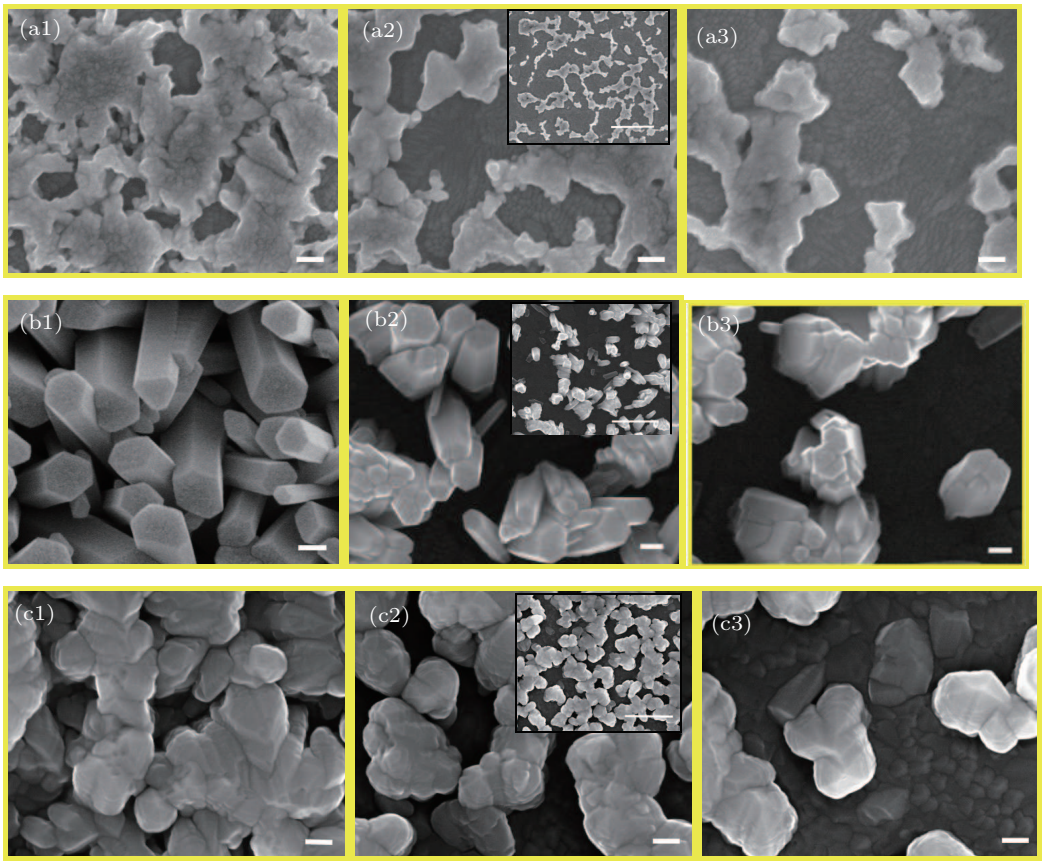


Fig. 2. (color online) (a1)–(a3) SEM images of seeding layer, (b1)–(b3) ZnO nanorods, and (c1)–(c3) modified ZnO nanorod. 1, 2, and 3 refer to the 5 min, 10 min, and 15 min etching time in NaOH solution (1 M). (Scale bars, 100 nm).

The wet-etching of the seed layer controls not only the spacing between the ZnO nanorods, but also the density of the nanorods. A shorter etching time makes the ZnO nanorods denser, and there is not enough spacing between them for the subsequent a-Si:H to form solar cells with 3D nanostructure; whereas a longer etching time results in a lower density of ZnO nanorods, which provides enough space to form solar cells with 3D nanostructure. Depending on the silicon layer thickness in the solar cells, a proper etching time is important for optimizing the ZnO nanorod density. In this paper, a 10-min etching time is optimal and, thus, we select this etching time to make the ZnO nanorod-based transparent conductive oxide (TCO) electrode for a-Si:H solar cell depositions.

Figure 3 shows the schematic illustration of the a-Si:H

single-junction solar cell with 3D nanostructure. In order to know the performance of the a-Si:H single-junction solar cells, three types of solar cells are fabricated. A planar reference cell is deposited on planar glass coated with indium-tin-oxide (ITO) film and the AZO seeding layer, as shown in Fig. 4(a). The ZnO nanorod cell (Fig. 4(b)) is built on a planar glass coated with ITO film, wet-etched AZO seeding layer, and ZnO nanorods. The modified ZnO nanorod cell (Fig. 4(c)) is deposited on a planar glass coated with ITO film, wet-etched AZO seeding layer, ZnO nanorod, and 180-nm thick sputtered AZO. AFM images of the above a-Si:H solar cells are shown in Figs. 4(d)–4(f), respectively, showing that the surface morphology of the solar cell on the planar substrate is relatively smooth, whereas the nanorod cell and the modified nanrorod cell have nanodome-like surface morphologies. The SEM image in Fig. 4(g) shows additional details of the modified ZnO nanorod solar cell.

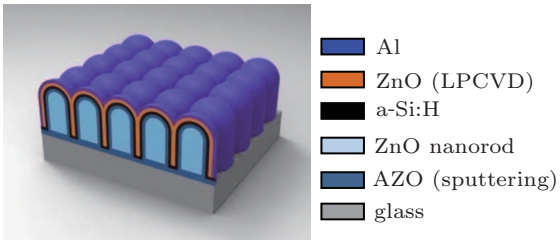


Fig. 3. (color online) Schematic illustration of the 3D a-Si:H single junction solar cell.

The measured J–V curves and solar cell characteristic parameters are shown in Fig. 5(a) and Table 1, respectively. Figure 5(a) shows a comparison among the J–V curves of solar cells deposited on the three types of substrates. The data in Table 1 show that the modified ZnO nanorod solar cell has an energy conversion efficiency of 7.03%, which is higher than the 6.43% and 4.27% achieved for the reference cell and the ZnO nanorod cell. The J_{sc} obtained from the planar cell is 12.70 mA/cm^2; whereas the J_{sc} values of the nanorod and modified nanorod solar cells are 14.22 mA/cm^2 and 15.43 mA/cm^2, respectively. Compared with the J_{sc} value of the planar reference cell, the J_{sc} values are increased by 12.7% and 22.0% for the nanorod cell and the modified nanorod cell, respectively. The EQE (Fig. 5(b)) of the nanorod cell is higher than that of the planar device in a wide wavelength range between 350 nm and 750 nm, except for the interference around 600 nm. The enhanced EQE in this wavelength range is mainly attributed to improved antireflection performance and enhanced absorption by effective light trapping in the semiconductor layer.[23,24]

In order to quantitatively characterize the absorptions of these solar cells, we carry out absolute hemispherical measurements with an integrating sphere. The reflection measurement is carried out in a broad range of wavelengths (300 nm–800 nm). The measured results are summarized in Fig. 5(c). Between 350 nm and 800 nm, the reflection of the modified nanorod solar cell is maintained to be lower than that of the nanorod solar cell. In addition, the reflection of the nanorod cell in a range of 600 nm–800 nm is lower than that of planar solar cell. As a result, the total absorption in the solar cells, represented as one minus the reflection from the solar cells (1-R), has the highest value for the modified nanorod solar cell.

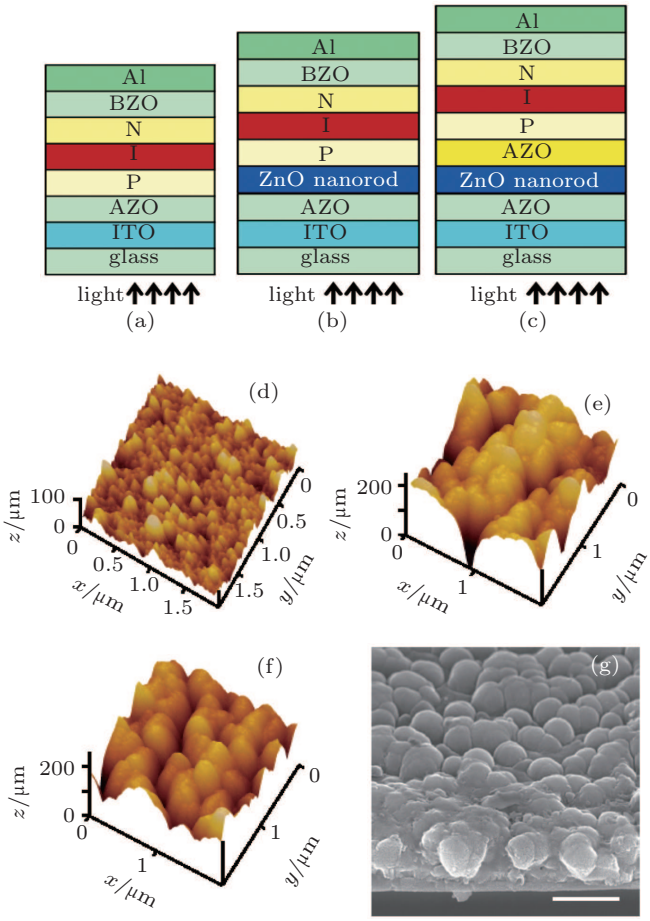


Fig. 4. (color online) Configurations, AFM images, SEM image of a-Si:H single junction solar cells: (a) configuration and (d) AFM image of the planar substrate device; (b) configuration and (e) AFM image of the ZnO nanorod substrate device; (c) configuration, (f) AFM image, and (g) SEM image (scale bar, 1.0 μm) of the modified ZnO nanorod substrate device.

Compared with the planar reference cell, the nanorod structured ZnO substrate cell has a 28% decrease in V_{oc}, which may be explained by two factors: an increased interface area between the nanorod front electrode and a-Si:H increases the dark current; and the ZnO nanorods have poor interface properties with a-Si:H, especially in the areas with no ZnO nanorods. Thus, the conversion efficiency of the nanorod cell is lower than that of the planar reference cell. The trade-off between optical and electrical properties is important for 3D solar cells. Generally, the V_{oc} of solar cells is not only determined by the bandgap of the intrinsic layer, but also limited by bulk and interface recombination.[25] For the planar reference cell, the bulk recombination could be a dominating factor for the V_{oc}, whereas for the nanorod cell, the interface

recombination could influence the V_{oc} due to an increased internal surface area and poorer interface properties.[26–28] The sharp edges and corners on the surfaces of the ZnO nanorods could cause the subsequently deposited solar cell to have a high defect density, and thus a low V_{oc}. This can be partly proved by increasing the dark saturation current density (J_0) from 3.0×10^{-4} A/cm^2 to 1.2×10^{-3} A/cm^2 (Table 1). This result demonstrates that the interface states are crucial for optimizing nanorod solar cells. In order to improve the interfaces of the nanorod solar cells, a 180-nm thick AZO film with high conductivity and transparency is deposited between the ZnO nanorod electrode and the p-type a-Si:H. This layer plays a role in modifying the ZnO nanorod surface to improve the interface contact by smoothing the sharp features. Compared with the nanorod cell, the modified nanorod cell has 16% increase in V_{oc} value, which is believed to be due to improved interfaces between the ZnO nanorods and a-Si:H p-layer, as supported by reducing the J_0 value from 1.2×10^{-3} A/cm^2 to 8.6×10^{-4} A/cm^2 (Table 1).

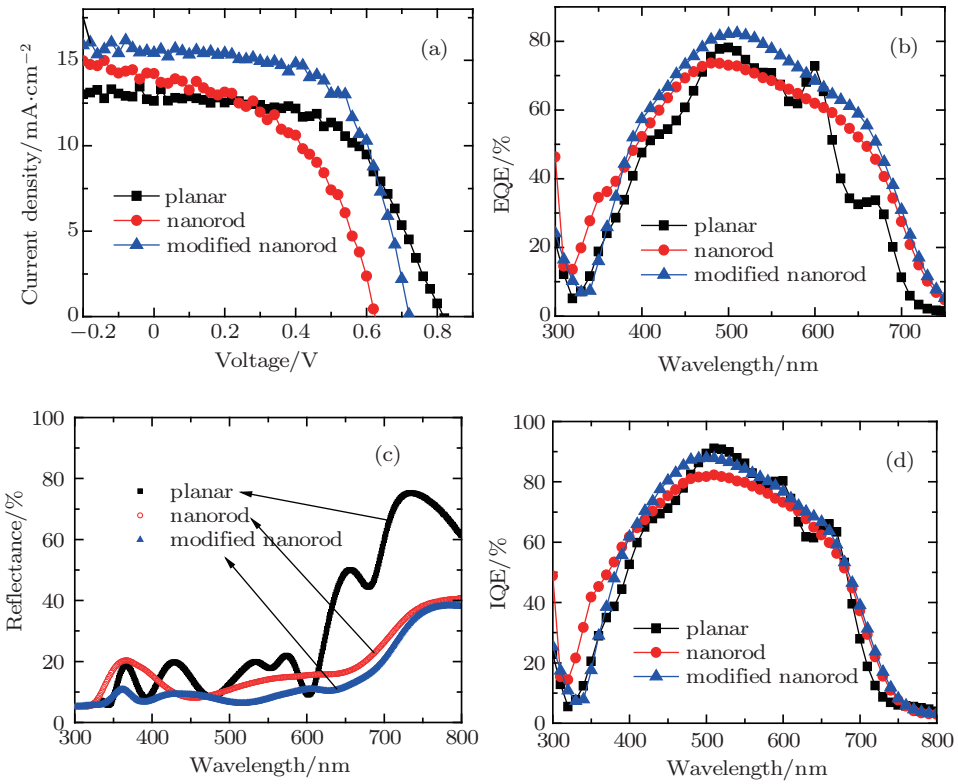


Fig. 5. (color online) (a) *J*–*V* characteristic curves, (b) EQE curves, (c) total device reflection curves, and (d) IQE curves of a-Si:H single junction solar cells deposited on planar, nanorod, and modified nanorod substrate, respectively.

Table 1. Characteristics of a-Si:H solar cells fabricated on planar, nanorod, and modified nanorod substrate.

Cell type	J_{sc}/(mA/cm^2)	V_{oc}/V	FF	Eff./%	J_0/(A/cm^2)	R_s/Ω·cm^2	R_h/Ω·cm^2
Planar	12.62	0.864	0.59	6.43	3.0×10^{-4}	26.2	838
Nanorod	14.22	0.626	0.48	4.27	1.2×10^{-3}	10.7	204
Modified nanorod	15.43	0.723	0.63	7.03	8.6×10^{-4}	9.2	383

The ZnO nanorods led to a 19% decrease in the FF compared with the FF value in the planar reference cell, which can be attributed to the decrease of the shunt resistance (R_h) from 838 Ω·cm^2 to 204 Ω·cm^2. However, the modified nanorod cell shows a 6.8% increase in FF, arising from the decrease of the series resistance (R_s) from 26.2 Ω·cm^2 to 9.2 Ω·cm^2 as shown in Table 1. One reason is that the low series resistance could result from a smaller average thickness for the 3D nanostructured solar cell than the planar solar cell, even when prepared with the same PECVD process. Another reason is likely to be that the interface is improved by adding the sputtering AZO covering layer.

The improvement in the cell performance is mainly from the photocurrent increase, which could be due to effective light trapping and improved carrier collection. Therefore, it is important to understand the carrier collection. The EQE is based

on spectrally resolved photocurrent measured under zero external bias and represents the ratio of the number of photo carriers collected by an external circuit to the number of incident photons at a given wavelength. This includes the contribution of photons that never reach the active layer due to reflection and absorption in the inactive layers. In order to understand the difference between the carrier extraction mechanisms, the internal quantum efficiency (IQE) is determined by the equation IQE = EQE/(1 − $R(\lambda)$), where $R(\lambda)$ (Fig. 5(c)) is the reflectance at a wavelength of λ (measured using an integrating sphere to include diffuse reflectance). Figure 5(d) shows the calculated IQEs of the solar cells deposited on the three types of substrate. As a result, the modified nanorod cell shows the highest value of EQE. This means that the 3D a-Si:H solar cells deposited on the modified ZnO nanorods benefit not only from improved light absorption but also from increased carrier extraction. The principle of light absorption and carrier collection in this type of device is similar to that in Hsu *et al*.'s nanostructure,[1] Kelzenberg *et al*.'s Si nanowire arrays,[29] and Zhu *et al*.'s Si nanocone arrays.[30] The advantage of our ZnO nanorod substrate is that it is prepared using an inexpensive process that requires neither lithographic patterning nor catalysts for the growth of the nanorods. In particular, the structure of the cells is of a traditional superstrate (p–i–n), which is different from what are reported by Zhu *et al*.,[30] Kuang *et al*.,[31] and Ferry *et al*.[32] The p–i–n structured a-Si:H-based solar cells are widely used in solar panel production.

4. Conclusions

In this paper, the ZnO nanorod TCO is synthesized by a series of processes, which includes the ZnO seed layer deposition, wet-etching of the seeding layer, chemical bath deposition of the ZnO nanorods, and sputtering deposition of an AZO covering layer. The enhanced light absorption and effective carrier collection in the modified nanorod solar cell led to an improvement in energy conversion compared with the energy conversions of the planar reference cell and the nanorod cell. This simple and scalable fabrication process of the ZnO nanorods without lithographic pattering turns our process of fabricating randomly oriented and modified ZnO nanorods into a great potential for use in low cost and high efficiency a-Si:H solar panel production.

Acknowledgment

The authors would like to thank Yang Xu and Zhao Hui-Xu for fabricating the ZnO:B by LPCVD, and also thank Yan Bao-Jie and Laura Sivec for improving the manuscript.

References

[1] Hsu M C, Battaglia C, Pahud C, Ruan Z C, Haug F J, Fan S H, Ballif C and Cui Y 2012 *Adv. Mater.* **2** 628
[2] Fan Z Y, Azavi H, Do J W, Moriwaki A, Ergen O, Chueh Y L, Leu P W, Ho J C, Takahashi T, Reichertz L A, Neale S, Yu K, Wu M, Ager J W and Javey A 2009 *Nat. Mater.* **8** 648
[3] Bai A Q, Zheng J, Tao Y L, Zuo Y H, Xue C L, Cheng B W and Wang Q M 2011 *Chin. Phys. B* **20** 116103
[4] Jeong S, Hu L, Lee H R, Garnett E, Choi J W and Cui Y 2010 *Nano Lett.* **10** 2989
[5] Kim J, Hong A J, Nah J W, Shin B, Ross F M and Sadana D K 2012 *ACS Nano.* **6** 265
[6] Zhou H J, Wissinger M, Fallert J, Hauschild R and Stelzl F 2007 *Phys. Lett.* **91** 181112
[7] Wang X D, Summers C J and Wang Z L 2004 *Nano Lett.* **4** 423
[8] Yang C J, Wang S M and Liang S W 2007 *Appl. Phys. Lett.* **90** 033104
[9] Battaglia C, Hsu C M, Söderström K, Escarré J, Haug F J, Charrière M, Boccard M, Despeisse M, Alexander D T L, Cantoni M, Cui Y and Ballif C 2012 *ACS Nano.* **6** 2790
[10] Lin A and Phillips J 2008 *Sol. Energy Mater. Sol. Cells* **92** 1689
[11] Niederberger M and Cölfen H 2006 *Phys. Chem. Chem. Phys.* **8** 3271
[12] Liu D F, Xiang Y J, Wu X C, Zhang Z X, Liu L F, Song L, Zhao X W, Luo S D, Ma W J, Shen J, Zhou W Y, Wang G, Wang C Y and Xie S S 2006 *Nano Lett.* **6** 2375
[13] Huang M H, Mao S, Feick H, Yan H, Wu Y, Kind H, Weber E, Russo R and Yang P D 2001 *Science* **292** 1897
[14] Pan N, Xue H, Yu M, Cui X, Wang X, Hou G, Huang J and Deng S Z 2010 *Nanotechnology* **21** 225707
[15] Li Y B, Pan H, Lin J Y, Ding J, Feng Y P, Thongmee S, Liu T, Gong H and Wang L 2008 *Adv. Mater.* **20** 1170
[16] Erdélyi R, Nagata T, Rogers D J, Teherani F H, Horváth Z E, Lábadi Z, Baji Z, Wakayam Y and Volk J 2011 *Cryst. Growth Des.* **11** 2515
[17] Qin Y, Wang X and Wang Z L 2008 *Nature* **451** 809
[18] Lee Y J, Sounart T L, Liu J, Spoerke E D, McKenzie B B, Hsu J W P and Voigt J A 2008 *Cryst. Growth Des.* **8** 2036
[19] Law M, Greene L E, Johnson J C, Saykally R and Yang P D 2005 *Nat. Mater.* **4** 455
[20] Yu M, Long Y Z, Sun B and Fan Z Y 2012 *Nanoscale* **4** 2783
[21] Xu C and Wang Z L 2011 *Adv. Mater.* **23** 873
[22] Greene L E, Law M, Tan D H, Montano M, Goldberger J, Somorjai G and Yang P D 2005 *Nano Lett.* **5** 1231
[23] Ferry V E, Verschuuren M A, Li H B T, Verhagen E, Walters R J, Schropp R E I, Atwater H A and Polman A 2010 *Opt. Express* **18** A237
[24] Spinelli P, Verschuuren M A and Polman A 2012 *Nat. Commun.* **3** 692
[25] Green M A 1982 *Solar Cells: Operating Principles, Technology, and System Applications* (New Jersey: Prentice-Hall)
[26] Kieven D, Dittrich T, Belaidi A, Tornow J, Schwarzburg K, Allsop N and Lux-Steiner M 2008 *Appl. Phys. Lett.* **92** 153107
[27] Spurgeon J M, Atwater H A and Lewis N S 2008 *J. Phys. Chem. C* **112** 6186
[28] Krunks M, Kärber E, Katerski A, Otto K, Acik I O, Dedova T and Mere A 2010 *Sol. Energy Mater. Sol. Cells* **94** 1191
[29] Kelzenberg M D, Boettcher S W, Petykiewicz J A, Turner-Evans D B, Putnam M C, Warren E L, Spurgeon J M, Briggs R M, Lewis N S and Atwater H A 2010 *Nat. Mater.* **9** 239
[30] Zhu J, Yu Z, Burkhard G F, Hsu C M, Connor S T, Xu Y, Wang Q, Mc Gehee M, Fan S and Cui Y 2009 *Nano Lett.* **9** 279
[31] Kuang Y, Werf K H M, Houweling Z S and Schropp R E I 2011 *Appl. Phys. Lett.* **98** 113111
[32] Ferry V E, Verschuuren M A, Lare M C, Schropp R E I, Atwater H A and Polman A 2011 *Nano Lett.* **11** 4239